Armstrong Aimee (Orcid ID: 0000-0002-4534-5075)
Zampi Jeffrey (Orcid ID: 0000-0002-5865-9591)
Benson Lee (Orcid ID: 0000-0002-1407-1825)

Use of 3D Rotational Angiography to Perform Computational Fluid Dynamics and Virtual Interventions in Aortic Coarctation

Aimee K. Armstrong, MD[1], Jeffrey D. Zampi, MD[2], Lucian M. Itu, PhD[3], Lee N. Benson, MD[4]

[1]The Heart Center, Nationwide Children's Hospital, Columbus, Ohio; [2]The Division of Pediatric Cardiology, University of Michigan, Ann Arbor, Michigan; [3]Department of Corporate Technology, Siemens SRL, Brasov, Romania and Department of Automation and Information Technology, Transylvania University of Brasov, Brasov, Romania; [4]The Division of Cardiology, The Labatt Family Heart Center, The Hospital for Sick Children, Toronto, Canada

Work Performed At: University of Michigan C.S. Mott Children's Hospital, The Hospital for Sick Children

Indexing Words: congenital heart disease, coarctation, pediatrics

Address for Correspondence:

Aimee K. Armstrong, MD, FAAP, FACC, FSCAI
Professor of Pediatrics, The Ohio State University
Nationwide Children's Hospital
700 Children's Drive
Columbus, OH 43205-2664
Fax: 614-722-5030
Phone: 614-722-2537
Aimee.Armstrong@nationwidechildrens.org

Short title: Computational Fluid Dynamics Using 3DRA

Total word count: 3,050

Abstract

Computational fluid dynamics (CFD) can be used to analyze blood flow and to predict hemodynamic outcomes after interventions for coarctation of the aorta and other cardiovascular diseases. We report the first use of cardiac 3-dimensional rotational angiography for CFD and show not only feasibility but also validation of its hemodynamic computations with catheter-based measurements in 3 patients.

Introduction

Aortic coarctation occurs in 5–8% of patients with congenital heart disease and causes upper-body hypertension and long-term sequelae, including persistent hypertension, stroke, coronary artery disease, aneurysm formation, and decreased life expectancy (1, 2). Treatment is recommended for a peak systolic gradient (PSG) of 20 mmHg and is reasonable for less than 20 mmHg, if there is systemic hypertension (3). In older children through adults, stent therapy is becoming standard of care (4).

The morphology of coarctation ranges from a discrete lesion, commonly at the aortic isthmus, to diffuse arch hypoplasia. This diversity results in a patient-specific anatomical and hemodynamic environment. The presence of any degree of transverse arch hypoplasia complicates the decision making process for treatment, such that it is unclear if stenting the isthmus lesion will achieve adequate gradient reduction. Even mild residual hypoplasia can cause long-term sequelae and

increase the risk of chronic hypertension (5). As such, management requires an individualized treatment plan to obtain the best physiologic result. At present, however, standard imaging techniques and hemodynamic assessment at catheterization cannot predict the post-stent hemodynamic outcome. In this regard, computational fluid dynamics (CFD) techniques, in combination with virtual stenting, may enable treatment to be individualized and the physiological results to be anticipated before actually performing the intervention.

CFD uses computer-based simulation to analyze fluid flow and has been used for decades to analyze blood flow in the cardiovascular system, particularly in the coronary arteries, the aorta, and single ventricle heart disease (6, 7, 8). While CFD is approved for clinical use in coronary artery disease, it is not routinely used in congenital heart disease for diagnosis or clinical decision making (9). Clinical data supporting accuracy of CFD in congenital heart disease are emerging. Early work using magnetic resonance imaging (MRI) and computed tomography angiography (CTA)-based CFD to predict invasively obtained gradients non-invasively in coarctation patients has been described (10,11). While CFD will likely find clinical applicability in avoiding invasive catheterization for pressure gradient measurements in the future, CFD could also be used in the cardiac catheterization laboratory (CCL) for virtual interventions and predictive modeling to individualize interventions during the catheterization procedure, without a preceding MRI or CTA.

In this case series, we utilize a new technology to allow CFD to be performed using data obtained solely in the CCL, without the need for MRI, CTA, or other pre-operative imaging. This technology uses an angiographic CT or CT-like image obtained from 3-dimensional rotational angiography (3DRA), specifically a DynaCT acquisition system (Siemens Healthcare GmbH, Erlangen, Germany). Due to the computational speed of this unique CFD model, use of 3DRA for CFD could allow for complete hemodynamic assessment, virtual interventions and predictive modeling, all while the patient is in the CCL, prior to performing the clinical intervention. In the future, this would allow for treatment planning to be personalized for each patient, including stent length, diameter, and location.

We sought to test the feasibility of using data obtained solely in the CCL for CFD in 3 patients undergoing coarctation stenting and compared the PSG computed by CFD before and after virtual stenting with that obtained directly by catheter before and after actual stent implantation. As this was performed to test feasibility, the CFD was run after the procedure, and clinical decisions were not based on the results. We hypothesized that the new CFD model would calculate PSGs that would correlate with those obtained by direct catheter measurement with an absolute error of <5 mmHg, which has been shown when comparing catheter-derived gradients to MRI-based CFD-derived gradients (10,11). We are the first to report cardiac CFD being performed from 3DRA and catheterization hemodynamic data alone.

Case Series

Clinical Protocol

Written informed consent was obtained from the patients' guardians. The study was approved by the Institutional Review Board of the two participating centers. Cardiac catheterization was performed using a biplane Siemens Artis Zee angiographic system (Siemens Healthcare GmbH, Erlangen, Germany). General anesthesia was used for all patients. Prior to stenting, a complete hemodynamic catheterization was performed, including thermodilution cardiac output (TDCO) measurements. Using a 3.5F Millar Mikro-Cath™ Diagnostic Pressure Catheter (Millar Inc., Houston, TX) through a guide catheter, pressures were obtained in the left ventricle, ascending aorta just above the aortic valve, innominate artery, left carotid artery, left subclavian artery, and descending aorta at the level of the diaphragm.

A pre-stent 3DRA was performed with a 6F pigtail catheter in the left ventricle. A contrast mixture of 50% contrast (contrast type and dose were institutional standard for 3D) and 50% saline was injected over 7 seconds with a 2 second x-ray delay and a 5-second spin. During injection, rapid right ventricular pacing at 180-240 paces per minute was performed to decrease the systolic blood pressure by 50%, and a breath hold was performed to minimize motion artifact. A low dose spin protocol was used (12 mGy/frame, 1.5 degrees per frame, 30 frames per second). The 2D biplane aortic angiogram was used, when available, to determine pulsatility of the aorta for elasticity assessment. Aortic coarctation stenting was performed at the operators'

discretion. A post-stent 3DRA was performed, using the same protocol as for the pre-stent 3DRA, and a hemodynamic catheterization was repeated.

CFD Technical Protocol

The CFD model uses a reduced order formulation of the equations of fluid flow that is designed to provide accurate representation of cross-section averaged quantities, such as pressure loss and flow in each branch, while sacrificing the ability to capture local flow variations. The model has the advantage of being rapid enough to be valuable as a clinical application, taking an average of 3 minutes of computation time per patient, compared to several hours for typical CFD simulators. The model is described in more detail in previous publications (10), where it is shown to provide good predictions of catheter-measured PSG based on MR and phase-contrast imaging derived flow rates. Specifically, the reduced-order multiscale fluid-structure interaction blood flow model is employed to compute pre- and post-stenting hemodynamics. It is based on a quasi one-dimensional model for the large arteries and a lumped parameter model (three-element Windkessel model), which accounts for the effect of the distal vasculature. To enable accurate pressure computation in the coarctation region, a locally defined pressure-drop model is embedded into the reduced-order blood flow model (12). Time-varying flow rate profiles are used as the inlet boundary condition. A parameter estimation framework is employed for personalizing the hemodynamic computations, comprising two calibration procedures, focusing on the cycle-averaged and time-dependent quantities.

In the current work, we extended this model to 3DRA for the anatomic assessment, using thermodilution cardiac output to set the inlet boundary condition. Invasively measured pressures in the ascending aorta, along with angiographically measured aortic diameters, were used to personalize the model parameters, and the PSG across the coarctation was then computed. The coarctation geometry was modified to simulate the effect of stenting. The virtual stent location was chosen independently from the actual stenting procedure. The stent length and diameter were chosen to relieve all stenosis in the descending thoracic aorta, matching the diameter of the stent to the aortic diameter on either end of the virtual stent. There were no significant differences in the post-stenting actual and predicted anatomical configurations. A post-stent PSG was computed, using the same flowrate and personalized model properties as the pre-stent computations, in order to simulate real-time work in the CCL (Figure 1). The computational run times for the three cases were 147, 190, and 176 seconds (mean time 171 ± 22 seconds).

Case 1

A 13-year-old 55.5 kg female was referred to the CCL for a severe native coarctation of the aorta with an arm-leg cuff PSG of 56 mmHg with upper extremity hypertension (146/52 mmHg). Catheterization revealed a discrete, severe coarctation distal to the left subclavian artery. PSG was 41 mmHg with a TDCO of 4.7 L/min (Table I), and the CFD processor predicted a PSG of 40 mmHg. The coarctation was treated with a 36 mm long Cheatham Platinum (CP) stent

(NuMED, Hopkinton, NY) mounted on a 12 mm Z-Med II-X balloon catheter (NuMED, Hopkinton, NY). The residual PSG across the arch was 14 mmHg, and virtual stenting predicted a residual PSG of 10 mmHg (Figure 2 and Table II).

Case 2

A 16-year-old 69.6 kg male came to the CCL for treatment of a native coarctation of the aorta, due to an arm-leg cuff PSG of 50 mmHg with upper extremity hypertension (150/82 mmHg). He also had a bicuspid aortic valve, mild aortic regurgitation, and a dilated aortic root. Catheterization showed a moderate, discrete coarctation distal to the left subclavian artery with a PSG of 29 mmHg and TDCO of 5.7 L/min. CFD predicted a PSG of 29 mmHg. The coarctation was treated with a 45 mm long CP stent mounted on a 15 mm Z-Med II-X balloon catheter. The residual PSG was 3 mmHg, and, after virtual stenting, the PSG was computed as 2 mmHg (Figure 3 and Table II).

Case 3

A 10-year-old 34.8 kg female underwent catheterization for a native coarctation of the aorta, due to an arm-leg cuff PSG of 32 mmHg without upper extremity hypertension. A mild, discrete coarctation in the mid-thoracic descending aorta resulted in a PSG of 19 mmHg with a TDCO of 3.9 L/min. CFD computed a PSG of 18 mmHg. The coarctation was treated with a 39 mm long covered CP stent mounted on a 16 mm Balloon in Balloon catheter (NuMED, Hopkinton, NY).

There was no residual gradient from ascending aorta to descending aorta at catheterization and or in the model with virtual stenting (Figure 4 and Table II).

Discussion

Since the 1990s, MRI-based CFD advanced from a preclinical modality to clinical application by evaluating pathophysiology, surgical and catheter-based treatment planning, and outcome prediction. However, clinical data to prove the accuracy of the data obtained from CFD in congenital heart disease are still limited. Aside from case reports, two studies have compared catheter-based and CFD-based gradients before and after aortic stenting and virtual stenting, respectively. First, Goubergrits *et al* evaluated 13 patients who underwent catheterization and preceding MRI, 1 day to 4 weeks apart, for coarctation of the aorta (11). MRI included 3D whole-heart and flow-sensitive 4D velocity-encoded sequences (Gyrotools, Zurich, Switzerland). CFD assessments were performed using Fluent® 6.3.26 (Ansys, Canonsburg, PA), and the post-treatment aortic geometry was virtually reconstructed from x-ray images. Pre-stent PSGs measured by catheter- and MRI-based CFD correlated significantly with a correlation coefficient of 0.97 and an absolute error of -0.5±0.33 mmHg. Post-stent PSGs also correlated significantly with a correlation coefficient of 0.87 and absolute error of 3.0±2.91 mmHg (11).

Second, Ralovich *et al* investigated data sets from 6 coarctation patients who had undergone pre- and post-intervention MRI and catheterizations (10). Using MRI-based CFD and virtual stenting,

there was good agreement between CFD computed PSGs and catheter PSGs with an average absolute error of 2.38±0.82 mmHg (pre-stenting), 1.10±0.63 mmHg (post-stenting), and 4.99±3.00 mmHg (virtual stenting).

To date, 3DRA-based CFD has been used clinically to understand the hemodynamics of brain aneurysms and to aid in treatment planning but has not been used in cardiac disease. Because of its high spatial resolution, low sensitivity to patient motion, and low visibility of bone, 3DRA has been used as the imaging gold standard when comparing CFD using MRI and CTA (13). Our first use of this imaging modality to perform cardiac CFD not only shows feasibility but also begins to validate its hemodynamic computations with catheter-based measurements, as all the gradients were within 5 mmHg of absolute error.

While CFD predicted the gradients with minimal absolute error, the post-stenting absolute pressures were not predicted accurately in all cases. The personalization for both the pre- and virtual post-stenting CFD based computations was performed using solely pre-stenting hemodynamic measurements, in order to mimic predictive modeling used real-time in the catheterization laboratory, during which only pre-stent hemodynamics would be available. For example, in Case #1, the patient's hemodynamics changed quite significantly between the pre- and post-stent settings (Table I) with the ascending aortic pressure and TDCO decreasing after stent placement. Despite using the pre-stent hemodynamics in the model, a prediction error of 4

mmHg indicated that the PSG prediction was quite robust and that its accuracy was only marginally affected by the change in post-stent hemodynamics.

3DRA-based cardiac CFD is the first step to perform virtual interventions real-time in the CCL and to allow CFD to guide management decisions during cardiac catheterization. Previous cardiac predictive modeling has used pre-procedural MRI or CTA (14,15). Our novel workflow could allow for CFD-guided personalized management decisions even when pre-procedural advanced imaging is not performed (14,15).

Limitations

The small prediction error (<5 mmHg) is one limitation of CFD, and a detailed uncertainty quantification analysis is planned for future studies. Error can come from modeling assumptions, anatomical reconstruction errors, inaccurate elastic wall modeling, and inaccuracies in the physiological measurements, such as thermodilution cardiac output. The reduced-order multiscale model is also limited by its inability to produce 3D streamlines, vortices, and wall shear stress. It was chosen for performing the blood flow computations, mainly due to the significantly reduced computation time, with an aim of running the calculations real-time, while the patient is on the catheterization table.

Conclusion

The ability to have patient-specific predictive modeling with hemodynamic assessment in the CCL will allow clinical decisions regarding stent therapy to be based on robust data, as opposed to guessing and assumptions, as it is done now. This may revolutionize the way we make clinical decisions and significantly improve care, if this can be done real-time during the catheterization. Widespread use of this technology will require large-scale studies to assure reliability and validity and to move CFD assessment into the CCL.

References

1. Baumgartner H, Bonhoeffer P, De Groot N, de Haan F, Deanfield J, Galie N, Gatzoulis M, Gohlke-Baerwolf C, Kaemmerer H, Kilner P, Meijboom F, Mulder B, Oechslin E, Oliver J, Serraf A, Szatmari A, Thaulow E, Vouhe P, Walma E. ESC Guidelines for the management of grown-up congenital heart disease (new version 2010). *Eur Heart J* 2010;31:2915–2957. doi: 10.1093/eurheartj/ehq249.

2. Bouchart F, Dubar A, Tabley A, Litzler P, Haas-Hubscher C, Redonnet M, Bessou J, Soyer R. Coarctation of the Aorta in Adults: Surgical Results and Long-Term Follow-up. *Ann Thorac Surg* 2000;79:1483-1488.

3. Feltes T, Bacha E, Beekman R, Cheatham J, Feinstein J, Gomes A, Hijazi Z, Ing F, de Moor M, Morrow W, Mullins C, Taubert K, Zahn E. Indications for cardiac catheterization and intervention in pediatric cardiac disease: a scientific statement from the American Heart Association. *Circulation* 2011;123:2607-2652. doi: 10.1161/CIR.0b013e31821b1f10.

4. Meadows J, Minahan M, McElhinney DB, McEnaney K, Ringel R; on behalf of the COAST Investigators. Intermediate Outcomes in the Prospective, Multicenter Coarctation of the Aorta Stent Trial (COAST). *Circulation* 2015;131:1656-1664. doi: 10.1161/CIRCULATIONAHA.114.013937.

5. Quennelle S, Powell A, Geva T, Prakash A. Persistent aortic arch hypoplasia after coarctation treatment is associated with late systemic hypertension. *J Am Heart Assoc* 2015;4:1-8. doi: 10.1161/JAHA.115.001978.

6. Lee BK. Computational Fluid Dynamics in Cardiovascular Disease. *Korean Circ J* 2011;41:423-430. doi: 10.4070/kcj.2011.41.8.423.

7. Pennati G, Corsini C, Hsia T-Y, Migliavacca F, for the Modeling of Congenital Hearts Alliance (MOCHA) Investigators. Computational fluid dynamics models and congenital heart diseases. *Front Pediatr* 2013;1:1-7. doi: 10.3389/fped.2013.00004.

8. Morris PD, Narracott A, von Tengg-Kobligk H, Soto DAS, Hsiao S, Lungu A, Evans P, Bressloff NW, Lawford PV, Hose DR, Gunn JP. Computational fluid dynamics modelling in cardiovascular medicine. *Heart* 2016;102:18-28. doi: 10.1136/heartjnl-2015-308044

9. Koo B, Erglis A, Doh J, Daniels D, Jegere S, Kim H, Dunning A, DeFrance T, Lansky A, Leipsic J, Min J. Diagnosis of Ischemia-Causing Coronary Stenoses by Noninvasive Fractional Flow Reserve Computed From Coronary Computed Tomographic Angiograms Results From the Prospective Multicenter DISCOVER-FLOW (Diagnosis of Ischemia-Causing Stenoses Obtained

Via Noninvasive Fractional Flow Reserve) Study. *J Am Coll Cardiol* 2011;58:1989–1997. doi: 10.1016/j.jacc.2011.06.066.

10. Ralovich K, Itu L, Vitanovski D, Sharma P, Ionasec R, Miahlef V, Krawtschuk W, Zheng Y, Everett A, Pongiglione G, Lenoardi B, Ringel R, Navab N, Heimann T, Comaniciu D. Noninvasive hemodynamic assessment, treatment outcome prediction and follow-up of aortic coarctation from MR imaging. *Med Phys* 2015;42:2143-56. doi: 10.1118/1.4914856.

11. Goubergrits L, Riesenkampff E, Yevtushenko P, Schaller J, Kertzscher U, Hennemuth A, Berger F, Schubert S, Kuehne T. MRI-Based CFD for Diagnosis and treatment Prediction: Clinical Validation Study in Patients with Coarctation of the Aorta. *J Magn Reson Imaging* 2015;41:909-916. doi: 10.1002/jmri.24639

12. Itu L, Sharma P, Ralovich K, Mihalef V, Ionasec R, Everett A, Ringel R, Kamen A, Comaniciu D. Non-invasive hemodynamic assessment of aortic coarctation: validation with in vivo measurements. *Ann Biomed Eng* 2013;41:669–681. doi: 10.1007/s10439-012-0715-0.

13. Ren Y, Chen G, Liu Z, Cai Y, Lu G, Li Z. Reproducibility of image-based computational models of intracranial aneurysm: a comparison between 3D rotational angiography, CT angiography and MR angiography. *BioMed Eng OnLine* 2016;15:50-64. doi: 10.1186/s12938-016-0163-4.

14. Capelli C, Sauvage E, Giusti G, Bosi GM, Ntsinjana H, Carminati M, Derrick G, Marek J, Khambadkone S, Taylor AM, Schievano S. Patient-specific simulations for planning treatment in congenital heart disease. *Interface Focus* 2018;8:20170021. doi: 10.1098/rsfs.2017.0021.

15. Kwon S, Feinstein JA, Dholaki RJ, LaDisa JF. Quantification of local hemodynamic alterations caused by virtual implantation of three commercially-available stents for the treatment of aortic coarctation. *Pediatr Cardiol* 2014;35:732-740. doi: 10.1007/s00246-013-0845-7.

Figure Legends

Figure 1: 3D Rotational Angiography Computational Fluid Dynamics Workflow: (a) 3D rotational angiogram (arrow showing discrete coarctation), (b) segmentation, (c) final 3D segmented model, (d) boundary conditions added, (e) gradient prediction, (f) virtual stent implantation with boundary conditions, and (g) post-stent gradient prediction

Asc, Ascending; Desc, Descending

Figure 2: Case 1 (a) Dyna CT reconstruction and (b) pressure predictions pre-stent and (c) post-stent

Asc, Ascending; Desc, Descending; CFD, Computational Fluid Dynamics; Meas, Measured

Figure 3: Case 2 (a) Dyna CT reconstruction and (b) pressure predictions pre-stent and (c) post-stent

Asc, Ascending; Desc, Descending; CFD, Computational Fluid Dynamics; Meas, Measured

Figure 4: Case 3 (a) Dyna CT reconstruction and pressure predictions (b) pre-stent and (c) post-stent

Asc, Ascending; Desc, Descending; CFD, Computational Fluid Dynamics; Meas, Measured

Table I. (A) Pre-stent and (B) post-stent physiologic and anatomical parameters measured at catheterization

A. Pre-stent

Case	AAo BP [mmHg]	DAo BP [mmHg]	TDCO* [l/min]	Heart rate [bpm]	Minimum coarctation diameter [mm]	AAO diameter [mm]
1	104/62	63/53	4.7	101	4.4	16
2	92/51	63/51	5.7	64	6.8	40
3	96/54	77/56	3.9	74	5.9	17

B. Post-stent

Case	AAo SBP [mmHg]	DAo SBP [mmHg]	TDCO* [l/min]
1	85/52	71/48	3.7
2	100/54	97/61	6.4
3	109/71	110/74	5.7

AAo, Ascending aorta
DAo, Descending aorta
BP, Blood pressure
TDCO, thermodilution cardiac output
*Pre-stent TDCO was used for post-stent CFD in order to simulate real-time workflow in the cardiac catheterization laboratory

Table II. Pre-stent and post-stent peak systolic gradients (mmHg) measured by direct catheterization pullback (ascending aortic systolic pressure – descending aortic systolic pressure) and by Computational Fluid Dynamics

	Pre-Stent		Post-Stent	
	Measured	**CFD***	**Measured**	**CFD***
Case 1	41	40	14	10
Case 2	29	29	3	2
Case 3	19	18	0	0

*CFD, Computational Fluid Dynamics

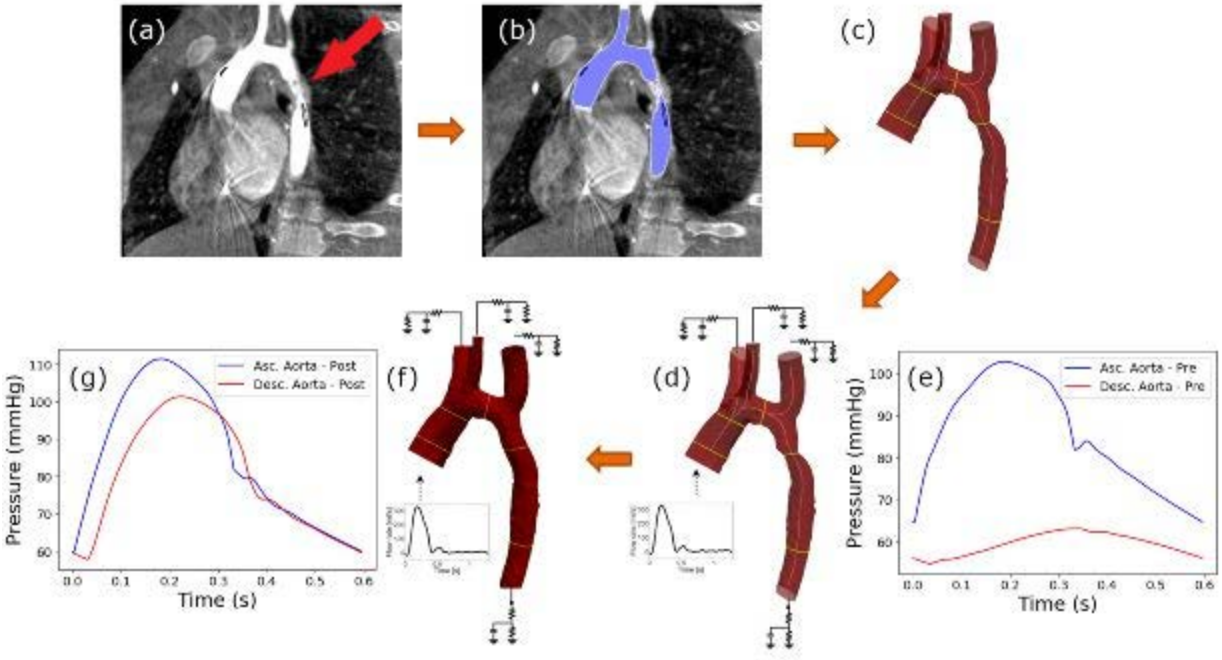

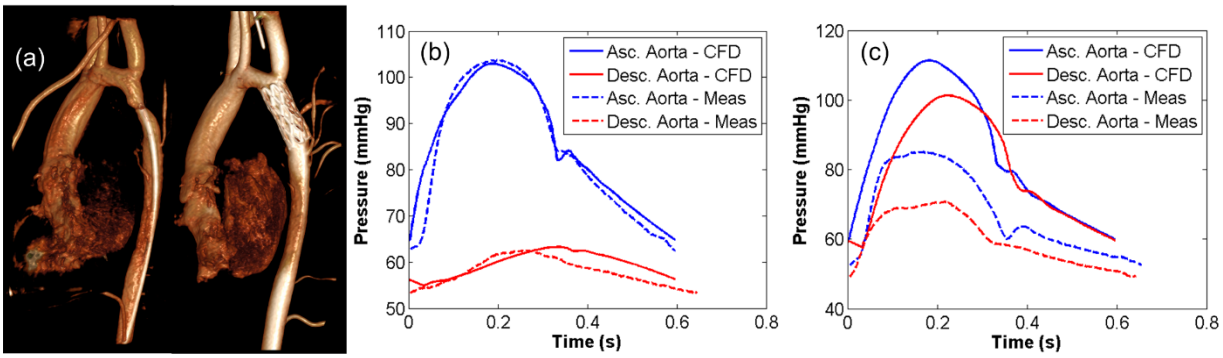

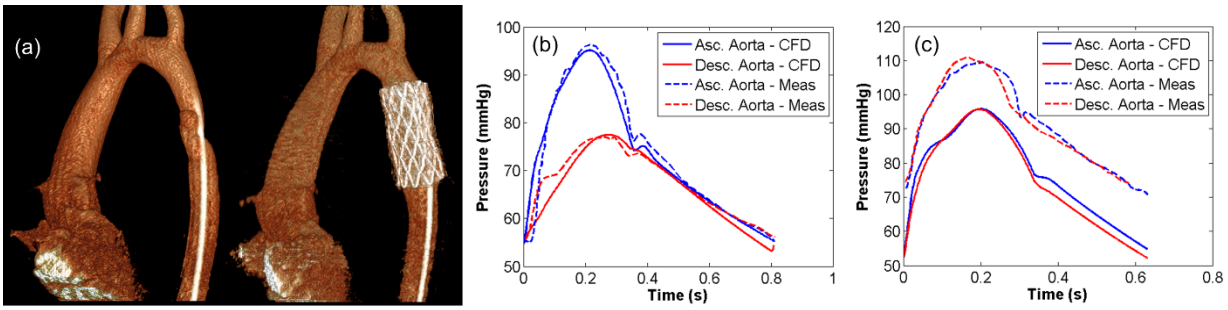

Use of 3D Rotational Angiography to Perform Computational Fluid Dynamics and Virtual Interventions in Aortic Coarctation

Short title: Computational Fluid Dynamics Using 3DRA

Total word count: 3,050

Abstract

Computational fluid dynamics (CFD) can be used to analyze blood flow and to predict hemodynamic outcomes after interventions for coarctation of the aorta and other cardiovascular diseases. We report the first use of cardiac 3-dimensional rotational angiography for CFD and show not only feasibility but also validation of its hemodynamic computations with catheter-based measurements in 3 patients.

Introduction

Aortic coarctation occurs in 5–8% of patients with congenital heart disease and causes upper-body hypertension and long-term sequelae, including persistent hypertension, stroke, coronary artery disease, aneurysm formation, and decreased life expectancy (1, 2). Treatment is recommended for a peak systolic gradient (PSG) of 20 mmHg and is reasonable for less than 20 mmHg, if there is systemic hypertension (3). In older children through adults, stent therapy is becoming standard of care (4).

The morphology of coarctation ranges from a discrete lesion, commonly at the aortic isthmus, to diffuse arch hypoplasia. This diversity results in a patient-specific anatomical and hemodynamic environment. The presence of any degree of transverse arch hypoplasia complicates the decision making process for treatment, such that it is unclear if stenting the isthmus lesion will achieve adequate gradient reduction. Even mild residual hypoplasia can cause long-term sequelae and increase the risk of chronic hypertension (5). As such, management requires an individualized treatment plan to obtain the best physiologic result. At present, however, standard imaging techniques and hemodynamic assessment at catheterization cannot predict the post-stent hemodynamic outcome. In this regard, computational fluid dynamics (CFD) techniques, in combination with virtual stenting, may enable treatment to be individualized and the physiological results to be anticipated before actually performing the intervention.

CFD uses computer-based simulation to analyze fluid flow and has been used for decades to analyze blood flow in the cardiovascular system, particularly in the coronary arteries, the aorta, and single ventricle heart disease (6, 7, 8). While CFD is approved for clinical use in coronary

artery disease, it is not routinely used in congenital heart disease for diagnosis or clinical decision making (9). Clinical data supporting accuracy of CFD in congenital heart disease are emerging. Early work using magnetic resonance imaging (MRI) and computed tomography angiography (CTA)-based CFD to predict invasively obtained gradients non-invasively in coarctation patients has been described (10,11). While CFD will likely find clinical applicability in avoiding invasive catheterization for pressure gradient measurements in the future, CFD could also be used in the cardiac catheterization laboratory (CCL) for virtual interventions and predictive modeling to individualize interventions during the catheterization procedure, without a preceding MRI or CTA.

In this case series, we utilize a new technology to allow CFD to be performed using data obtained solely in the CCL, without the need for MRI, CTA, or other pre-operative imaging. This technology uses an angiographic CT or CT-like image obtained from 3-dimensional rotational angiography (3DRA), specifically a DynaCT acquisition system (Siemens Healthcare GmbH, Erlangen, Germany). Due to the computational speed of this unique CFD model, use of 3DRA for CFD could allow for complete hemodynamic assessment, virtual interventions and predictive modeling, all while the patient is in the CCL, prior to performing the clinical intervention. In the future, this would allow for treatment planning to be personalized for each patient, including stent length, diameter, and location.

We sought to test the feasibility of using data obtained solely in the CCL for CFD in 3 patients undergoing coarctation stenting and compared the PSG computed by CFD before and after virtual stenting with that obtained directly by catheter before and after actual stent implantation.

As this was performed to test feasibility, the CFD was run after the procedure, and clinical decisions were not based on the results. We hypothesized that the new CFD model would calculate PSGs that would correlate with those obtained by direct catheter measurement with an absolute error of <5 mmHg, which has been shown when comparing catheter-derived gradients to MRI-based CFD-derived gradients (10,11). We are the first to report cardiac CFD being performed from 3DRA and catheterization hemodynamic data alone.

Case Series

Clinical Protocol

Written informed consent was obtained from the patients' guardians. The study was approved by the Institutional Review Board of the two participating centers. Cardiac catheterization was performed using a biplane Siemens Artis Zee angiographic system (Siemens Healthcare GmbH, Erlangen, Germany). General anesthesia was used for all patients. Prior to stenting, a complete hemodynamic catheterization was performed, including thermodilution cardiac output (TDCO) measurements. Using a 3.5F Millar Mikro-Cath™ Diagnostic Pressure Catheter (Millar Inc., Houston, TX) through a guide catheter, pressures were obtained in the left ventricle, ascending aorta just above the aortic valve, innominate artery, left carotid artery, left subclavian artery, and descending aorta at the level of the diaphragm.

A pre-stent 3DRA was performed with a 6F pigtail catheter in the left ventricle. A contrast mixture of 50% contrast (contrast type and dose were institutional standard for 3D) and 50% saline was injected over 7 seconds with a 2 second x-ray delay and a 5-second spin. During injection, rapid right ventricular pacing at 180-240 paces per minute was performed to decrease

the systolic blood pressure by 50%, and a breath hold was performed to minimize motion artifact. A low dose spin protocol was used (12 mGy/frame, 1.5 degrees per frame, 30 frames per second). The 2D biplane aortic angiogram was used, when available, to determine pulsatility of the aorta for elasticity assessment. Aortic coarctation stenting was performed at the operators' discretion. A post-stent 3DRA was performed, using the same protocol as for the pre-stent 3DRA, and a hemodynamic catheterization was repeated.

CFD Technical Protocol

The CFD model uses a reduced order formulation of the equations of fluid flow that is designed to provide accurate representation of cross-section averaged quantities, such as pressure loss and flow in each branch, while sacrificing the ability to capture local flow variations. The model has the advantage of being rapid enough to be valuable as a clinical application, taking an average of 3 minutes of computation time per patient, compared to several hours for typical CFD simulators. The model is described in more detail in previous publications (10), where it is shown to provide good predictions of catheter-measured PSG based on MR and phase-contrast imaging derived flow rates. Specifically, the reduced-order multiscale fluid-structure interaction blood flow model is employed to compute pre- and post-stenting hemodynamics. It is based on a quasi one-dimensional model for the large arteries and a lumped parameter model (three-element Windkessel model), which accounts for the effect of the distal vasculature. To enable accurate pressure computation in the coarctation region, a locally defined pressure-drop model is embedded into the reduced-order blood flow model (12). Time-varying flow rate profiles are used as the inlet boundary condition. A parameter estimation framework is employed for

personalizing the hemodynamic computations, comprising two calibration procedures, focusing on the cycle-averaged and time-dependent quantities.

In the current work, we extended this model to 3DRA for the anatomic assessment, using thermodilution cardiac output to set the inlet boundary condition. Invasively measured pressures in the ascending aorta, along with angiographically measured aortic diameters, were used to personalize the model parameters, and the PSG across the coarctation was then computed. The coarctation geometry was modified to simulate the effect of stenting. The virtual stent location was chosen independently from the actual stenting procedure. The stent length and diameter were chosen to relieve all stenosis in the descending thoracic aorta, matching the diameter of the stent to the aortic diameter on either end of the virtual stent. There were no significant differences in the post-stenting actual and predicted anatomical configurations. A post-stent PSG was computed, using the same flowrate and personalized model properties as the pre-stent computations, in order to simulate real-time work in the CCL (Figure 1). The computational run times for the three cases were 147, 190, and 176 seconds (mean time 171 ± 22 seconds).

Case 1

A 13-year-old 55.5 kg female was referred to the CCL for a severe native coarctation of the aorta with an arm-leg cuff PSG of 56 mmHg with upper extremity hypertension (146/52 mmHg). Catheterization revealed a discrete, severe coarctation distal to the left subclavian artery. PSG was 41 mmHg with a TDCO of 4.7 L/min (Table I), and the CFD processor predicted a PSG of 40 mmHg. The coarctation was treated with a 36 mm long Cheatham Platinum (CP) stent (NuMED, Hopkinton, NY) mounted on a 12 mm Z-Med II-X balloon catheter (NuMED,

Hopkinton, NY). The residual PSG across the arch was 14 mmHg, and virtual stenting predicted a residual PSG of 10 mmHg (Figure 2 and Table II).

Case 2

A 16-year-old 69.6 kg male came to the CCL for treatment of a native coarctation of the aorta, due to an arm-leg cuff PSG of 50 mmHg with upper extremity hypertension (150/82 mmHg). He also had a bicuspid aortic valve, mild aortic regurgitation, and a dilated aortic root. Catheterization showed a moderate, discrete coarctation distal to the left subclavian artery with a PSG of 29 mmHg and TDCO of 5.7 L/min. CFD predicted a PSG of 29 mmHg. The coarctation was treated with a 45 mm long CP stent mounted on a 15 mm Z-Med II-X balloon catheter. The residual PSG was 3 mmHg, and, after virtual stenting, the PSG was computed as 2 mmHg (Figure 3 and Table II).

Case 3

A 10-year-old 34.8 kg female underwent catheterization for a native coarctation of the aorta, due to an arm-leg cuff PSG of 32 mmHg without upper extremity hypertension. A mild, discrete coarctation in the mid-thoracic descending aorta resulted in a PSG of 19 mmHg with a TDCO of 3.9 L/min. CFD computed a PSG of 18 mmHg. The coarctation was treated with a 39 mm long covered CP stent mounted on a 16 mm Balloon in Balloon catheter (NuMED, Hopkinton, NY). There was no residual gradient from ascending aorta to descending aorta at catheterization and or in the model with virtual stenting (Figure 4 and Table II).

Discussion

Since the 1990s, MRI-based CFD advanced from a preclinical modality to clinical application by evaluating pathophysiology, surgical and catheter-based treatment planning, and outcome prediction. However, clinical data to prove the accuracy of the data obtained from CFD in congenital heart disease are still limited. Aside from case reports, two studies have compared catheter-based and CFD-based gradients before and after aortic stenting and virtual stenting, respectively. First, Goubergrits *et al* evaluated 13 patients who underwent catheterization and preceding MRI, 1 day to 4 weeks apart, for coarctation of the aorta (11). MRI included 3D whole-heart and flow-sensitive 4D velocity-encoded sequences (Gyrotools, Zurich, Switzerland). CFD assessments were performed using Fluent® 6.3.26 (Ansys, Canonsburg, PA), and the post-treatment aortic geometry was virtually reconstructed from x-ray images. Pre-stent PSGs measured by catheter- and MRI-based CFD correlated significantly with a correlation coefficient of 0.97 and an absolute error of -0.5±0.33 mmHg. Post-stent PSGs also correlated significantly with a correlation coefficient of 0.87 and absolute error of 3.0±2.91 mmHg (11).

Second, Ralovich *et al* investigated data sets from 6 coarctation patients who had undergone pre- and post-intervention MRI and catheterizations (10). Using MRI-based CFD and virtual stenting, there was good agreement between CFD computed PSGs and catheter PSGs with an average absolute error of 2.38±0.82 mmHg (pre-stenting), 1.10±0.63 mmHg (post-stenting), and 4.99±3.00 mmHg (virtual stenting).

To date, 3DRA-based CFD has been used clinically to understand the hemodynamics of brain aneurysms and to aid in treatment planning but has not been used in cardiac disease. Because of its high spatial resolution, low sensitivity to patient motion, and low visibility of bone, 3DRA has

been used as the imaging gold standard when comparing CFD using MRI and CTA (13). Our first use of this imaging modality to perform cardiac CFD not only shows feasibility but also begins to validate its hemodynamic computations with catheter-based measurements, as all the gradients were within 5 mmHg of absolute error.

While CFD predicted the gradients with minimal absolute error, the post-stenting absolute pressures were not predicted accurately in all cases. The personalization for both the pre- and virtual post-stenting CFD based computations was performed using solely pre-stenting hemodynamic measurements, in order to mimic predictive modeling used real-time in the catheterization laboratory, during which only pre-stent hemodynamics would be available. For example, in Case #1, the patient's hemodynamics changed quite significantly between the pre- and post-stent settings (Table I) with the ascending aortic pressure and TDCO decreasing after stent placement. Despite using the pre-stent hemodynamics in the model, a prediction error of 4 mmHg indicated that the PSG prediction was quite robust and that its accuracy was only marginally affected by the change in post-stent hemodynamics.

3DRA-based cardiac CFD is the first step to perform virtual interventions real-time in the CCL and to allow CFD to guide management decisions during cardiac catheterization. Previous cardiac predictive modeling has used pre-procedural MRI or CTA (14,15). Our novel workflow could allow for CFD-guided personalized management decisions even when pre-procedural advanced imaging is not performed (14,15).

Limitations

The small prediction error (<5 mmHg) is one limitation of CFD, and a detailed uncertainty quantification analysis is planned for future studies. Error can come from modeling assumptions, anatomical reconstruction errors, inaccurate elastic wall modeling, and inaccuracies in the physiological measurements, such as thermodilution cardiac output. The reduced-order multiscale model is also limited by its inability to produce 3D streamlines, vortices, and wall shear stress. It was chosen for performing the blood flow computations, mainly due to the significantly reduced computation time, with an aim of running the calculations real-time, while the patient is on the catheterization table.

Conclusion

The ability to have patient-specific predictive modeling with hemodynamic assessment in the CCL will allow clinical decisions regarding stent therapy to be based on robust data, as opposed to guessing and assumptions, as it is done now. This may revolutionize the way we make clinical decisions and significantly improve care, if this can be done real-time during the catheterization. Widespread use of this technology will require large-scale studies to assure reliability and validity and to move CFD assessment into the CCL.

References

1. Baumgartner H, Bonhoeffer P, De Groot N, de Haan F, Deanfield J, Galie N, Gatzoulis M, Gohlke-Baerwolf C, Kaemmerer H, Kilner P, Meijboom F, Mulder B, Oechslin E, Oliver J, Serraf A, Szatmari A, Thaulow E, Vouhe P, Walma E. ESC Guidelines for the management of grown-up congenital heart disease (new version 2010). *Eur Heart J* 2010;31:2915–2957. doi: 10.1093/eurheartj/ehq249.

2. Bouchart F, Dubar A, Tabley A, Litzler P, Haas-Hubscher C, Redonnet M, Bessou J, Soyer R. Coarctation of the Aorta in Adults: Surgical Results and Long-Term Follow-up. *Ann Thorac Surg* 2000;79:1483-1488.

3. Feltes T, Bacha E, Beekman R, Cheatham J, Feinstein J, Gomes A, Hijazi Z, Ing F, de Moor M, Morrow W, Mullins C, Taubert K, Zahn E. Indications for cardiac catheterization and intervention in pediatric cardiac disease: a scientific statement from the American Heart Association. *Circulation* 2011;123:2607-2652. doi: 10.1161/CIR.0b013e31821b1f10.

4. Meadows J, Minahan M, McElhinney DB, McEnaney K, Ringel R; on behalf of the COAST Investigators. Intermediate Outcomes in the Prospective, Multicenter Coarctation of the Aorta Stent Trial (COAST). *Circulation* 2015;131:1656-1664. doi: 10.1161/CIRCULATIONAHA.114.013937.

5. Quennelle S, Powell A, Geva T, Prakash A. Persistent aortic arch hypoplasia after coarctation treatment is associated with late systemic hypertension. *J Am Heart Assoc* 2015;4:1-8. doi: 10.1161/JAHA.115.001978.

6. Lee BK. Computational Fluid Dynamics in Cardiovascular Disease. *Korean Circ J* 2011;41:423-430. doi: 10.4070/kcj.2011.41.8.423.

7. Pennati G, Corsini C, Hsia T-Y, Migliavacca F, for the Modeling of Congenital Hearts Alliance (MOCHA) Investigators. Computational fluid dynamics models and congenital heart diseases. *Front Pediatr* 2013;1:1-7. doi: 10.3389/fped.2013.00004.

8. Morris PD, Narracott A, von Tengg-Kobligk H, Soto DAS, Hsiao S, Lungu A, Evans P, Bressloff NW, Lawford PV, Hose DR, Gunn JP. Computational fluid dynamics modelling in cardiovascular medicine. *Heart* 2016;102:18-28. doi: 10.1136/heartjnl-2015-308044

9. Koo B, Erglis A, Doh J, Daniels D, Jegere S, Kim H, Dunning A, DeFrance T, Lansky A, Leipsic J, Min J. Diagnosis of Ischemia-Causing Coronary Stenoses by Noninvasive Fractional Flow Reserve Computed From Coronary Computed Tomographic Angiograms Results From the Prospective Multicenter DISCOVER-FLOW (Diagnosis of Ischemia-Causing Stenoses Obtained Via Noninvasive Fractional Flow Reserve) Study. *J Am Coll Cardiol* 2011;58:1989–1997. doi: 10.1016/j.jacc.2011.06.066.

10. Ralovich K, Itu L, Vitanovski D, Sharma P, Ionasec R, Miahlef V, Krawtschuk W, Zheng Y, Everett A, Pongiglione G, Lenoardi B, Ringel R, Navab N, Heimann T, Comaniciu D. Noninvasive hemodynamic assessment, treatment outcome prediction and follow-up of aortic coarctation from MR imaging. *Med Phys* 2015;42:2143-56. doi: 10.1118/1.4914856.

11. Goubergrits L, Riesenkampff E, Yevtushenko P, Schaller J, Kertzscher U, Hennemuth A, Berger F, Schubert S, Kuehne T. MRI-Based CFD for Diagnosis and treatment Prediction: Clinical Validation Study in Patients with Coarctation of the Aorta. *J Magn Reson Imaging* 2015;41:909-916. doi: 10.1002/jmri.24639

12. Itu L, Sharma P, Ralovich K, Mihalef V, Ionasec R, Everett A, Ringel R, Kamen A, Comaniciu D. Non-invasive hemodynamic assessment of aortic coarctation: validation with in vivo measurements. *Ann Biomed Eng* 2013;41:669–681. doi: 10.1007/s10439-012-0715-0.

13. Ren Y, Chen G, Liu Z, Cai Y, Lu G, Li Z. Reproducibility of image-based computational models of intracranial aneurysm: a comparison between 3D rotational angiography, CT angiography and MR angiography. *BioMed Eng OnLine* 2016;15:50-64. doi: 10.1186/s12938-016-0163-4.

14. Capelli C, Sauvage E, Giusti G, Bosi GM, Ntsinjana H, Carminati M, Derrick G, Marek J, Khambadkone S, Taylor AM, Schievano S. Patient-specific simulations for planning treatment in congenital heart disease. *Interface Focus* 2018;8:20170021. doi: 10.1098/rsfs.2017.0021.

15. Kwon S, Feinstein JA, Dholaki RJ, LaDisa JF. Quantification of local hemodynamic alterations caused by virtual implantation of three commercially-available stents for the treatment of aortic coarctation. *Pediatr Cardiol* 2014;35:732-740. doi: 10.1007/s00246-013-0845-7.

Figure Legends

Figure 1: 3D Rotational Angiography Computational Fluid Dynamics Workflow: (a) 3D rotational angiogram (arrow showing discrete coarctation), (b) segmentation, (c) final 3D segmented model, (d) boundary conditions added, (e) gradient prediction, (f) virtual stent implantation with boundary conditions, and (g) post-stent gradient prediction

Asc, Ascending; Desc, Descending

Figure 2: Case 1 (a) Dyna CT reconstruction and (b) pressure predictions pre-stent and (c) post-stent

Asc, Ascending; Desc, Descending; CFD, Computational Fluid Dynamics; Meas, Measured

Figure 3: Case 2 (a) Dyna CT reconstruction and (b) pressure predictions pre-stent and (c) post-stent

Asc, Ascending; Desc, Descending; CFD, Computational Fluid Dynamics; Meas, Measured

Figure 4: Case 3 (a) Dyna CT reconstruction and pressure predictions (b) pre-stent and (c) post-stent

Asc, Ascending; Desc, Descending; CFD, Computational Fluid Dynamics; Meas, Measured

Use of 3D Rotational Angiography to Perform Computational Fluid Dynamics and Virtual Interventions in Aortic Coarctation

Aimee K. Armstrong, MD[1], Jeffrey D. Zampi, MD[2], Lucian M. Itu, PhD[3], Lee N. Benson, MD[4]

[1]The Heart Center, Nationwide Children's Hospital, Columbus, Ohio; [2]The Division of Pediatric Cardiology, University of Michigan, Ann Arbor, Michigan; [3]Department of Corporate Technology, Siemens SRL, Brasov, Romania and Department of Automation and Information Technology, Transylvania University of Brasov, Brasov, Romania; [4]The Division of Cardiology, The Labatt Family Heart Center, The Hospital for Sick Children, Toronto, Canada

Work Performed At: University of Michigan C.S. Mott Children's Hospital, The Hospital for Sick Children

Indexing Words: congenital heart disease, coarctation, pediatrics

Address for Correspondence:

Aimee K. Armstrong, MD, FAAP, FACC, FSCAI
Professor of Pediatrics, The Ohio State University
Nationwide Children's Hospital
700 Children's Drive
Columbus, OH 43205-2664
Fax: 614-722-5030
Phone: 614-722-2537
Aimee.Armstrong@nationwidechildrens.org

Short title: Computational Fluid Dynamics Using 3DRA

Total word count: 3,050

Abstract

Computational fluid dynamics (CFD) can be used to analyze blood flow and to predict hemodynamic outcomes after interventions for coarctation of the aorta and other cardiovascular diseases. We report the first use of cardiac 3-dimensional rotational angiography for CFD and show not only feasibility but also validation of its hemodynamic computations with catheter-based measurements in 3 patients.

Introduction

Aortic coarctation occurs in 5–8% of patients with congenital heart disease and causes upper-body hypertension and long-term sequelae, including persistent hypertension, stroke, coronary artery disease, aneurysm formation, and decreased life expectancy (1, 2). Treatment is recommended for a peak systolic gradient (PSG) of 20 mmHg and is reasonable for less than 20 mmHg, if there is systemic hypertension (3). In older children through adults, stent therapy is becoming standard of care (4).

The morphology of coarctation ranges from a discrete lesion, commonly at the aortic isthmus, to diffuse arch hypoplasia. This diversity results in a patient-specific anatomical and hemodynamic environment. The presence of any degree of transverse arch hypoplasia complicates the decision making process for treatment, such that it is unclear if stenting the isthmus lesion will achieve adequate gradient reduction. Even mild residual hypoplasia can cause long-term sequelae and increase the risk of chronic hypertension (5). As such, management requires an individualized treatment plan to obtain the best physiologic result. At present, however, standard imaging techniques and hemodynamic assessment at catheterization cannot predict the post-stent hemodynamic outcome. In this regard, computational fluid dynamics (CFD) techniques, in combination with virtual stenting, may enable treatment to be individualized and the physiological results to be anticipated before actually performing the intervention.

CFD uses computer-based simulation to analyze fluid flow and has been used for decades to analyze blood flow in the cardiovascular system, particularly in the coronary arteries, the aorta, and single ventricle heart disease (6, 7, 8). While CFD is approved for clinical use in coronary

artery disease, it is not routinely used in congenital heart disease for diagnosis or clinical decision making (9). Clinical data supporting accuracy of CFD in congenital heart disease are emerging. Early work using magnetic resonance imaging (MRI) and computed tomography angiography (CTA)-based CFD to predict invasively obtained gradients non-invasively in coarctation patients has been described (10,11). While CFD will likely find clinical applicability in avoiding invasive catheterization for pressure gradient measurements in the future, CFD could also be used in the cardiac catheterization laboratory (CCL) for virtual interventions and predictive modeling to individualize interventions during the catheterization procedure, without a preceding MRI or CTA.

In this case series, we utilize a new technology to allow CFD to be performed using data obtained solely in the CCL, without the need for MRI, CTA, or other pre-operative imaging. This technology uses an angiographic CT or CT-like image obtained from 3-dimensional rotational angiography (3DRA), specifically a DynaCT acquisition system (Siemens Healthcare GmbH, Erlangen, Germany). Due to the computational speed of this unique CFD model, use of 3DRA for CFD could allow for complete hemodynamic assessment, virtual interventions and predictive modeling, all while the patient is in the CCL, prior to performing the clinical intervention. In the future, this would allow for treatment planning to be personalized for each patient, including stent length, diameter, and location.

We sought to test the feasibility of using data obtained solely in the CCL for CFD in 3 patients undergoing coarctation stenting and compared the PSG computed by CFD before and after virtual stenting with that obtained directly by catheter before and after actual stent implantation.

As this was performed to test feasibility, the CFD was run after the procedure, and clinical decisions were not based on the results. We hypothesized that the new CFD model would calculate PSGs that would correlate with those obtained by direct catheter measurement with an absolute error of <5 mmHg, which has been shown when comparing catheter-derived gradients to MRI-based CFD-derived gradients (10,11). We are the first to report cardiac CFD being performed from 3DRA and catheterization hemodynamic data alone.

Case Series

Clinical Protocol

Written informed consent was obtained from the patients' guardians. The study was approved by the Institutional Review Board of the two participating centers. Cardiac catheterization was performed using a biplane Siemens Artis Zee angiographic system (Siemens Healthcare GmbH, Erlangen, Germany). General anesthesia was used for all patients. Prior to stenting, a complete hemodynamic catheterization was performed, including thermodilution cardiac output (TDCO) measurements. Using a 3.5F Millar Mikro-Cath™ Diagnostic Pressure Catheter (Millar Inc., Houston, TX) through a guide catheter, pressures were obtained in the left ventricle, ascending aorta just above the aortic valve, innominate artery, left carotid artery, left subclavian artery, and descending aorta at the level of the diaphragm.

A pre-stent 3DRA was performed with a 6F pigtail catheter in the left ventricle. A contrast mixture of 50% contrast (contrast type and dose were institutional standard for 3D) and 50% saline was injected over 7 seconds with a 2 second x-ray delay and a 5-second spin. During injection, rapid right ventricular pacing at 180-240 paces per minute was performed to decrease

the systolic blood pressure by 50%, and a breath hold was performed to minimize motion artifact. A low dose spin protocol was used (12 mGy/frame, 1.5 degrees per frame, 30 frames per second). The 2D biplane aortic angiogram was used, when available, to determine pulsatility of the aorta for elasticity assessment. Aortic coarctation stenting was performed at the operators' discretion. A post-stent 3DRA was performed, using the same protocol as for the pre-stent 3DRA, and a hemodynamic catheterization was repeated.

CFD Technical Protocol

The CFD model uses a reduced order formulation of the equations of fluid flow that is designed to provide accurate representation of cross-section averaged quantities, such as pressure loss and flow in each branch, while sacrificing the ability to capture local flow variations. The model has the advantage of being rapid enough to be valuable as a clinical application, taking an average of 3 minutes of computation time per patient, compared to several hours for typical CFD simulators. The model is described in more detail in previous publications (10), where it is shown to provide good predictions of catheter-measured PSG based on MR and phase-contrast imaging derived flow rates. Specifically, the reduced-order multiscale fluid-structure interaction blood flow model is employed to compute pre- and post-stenting hemodynamics. It is based on a quasi one-dimensional model for the large arteries and a lumped parameter model (three-element Windkessel model), which accounts for the effect of the distal vasculature. To enable accurate pressure computation in the coarctation region, a locally defined pressure-drop model is embedded into the reduced-order blood flow model (12). Time-varying flow rate profiles are used as the inlet boundary condition. A parameter estimation framework is employed for

personalizing the hemodynamic computations, comprising two calibration procedures, focusing on the cycle-averaged and time-dependent quantities.

In the current work, we extended this model to 3DRA for the anatomic assessment, using thermodilution cardiac output to set the inlet boundary condition. Invasively measured pressures in the ascending aorta, along with angiographically measured aortic diameters, were used to personalize the model parameters, and the PSG across the coarctation was then computed. The coarctation geometry was modified to simulate the effect of stenting. The virtual stent location was chosen independently from the actual stenting procedure. The stent length and diameter were chosen to relieve all stenosis in the descending thoracic aorta, matching the diameter of the stent to the aortic diameter on either end of the virtual stent. There were no significant differences in the post-stenting actual and predicted anatomical configurations. A post-stent PSG was computed, using the same flowrate and personalized model properties as the pre-stent computations, in order to simulate real-time work in the CCL (Figure 1). The computational run times for the three cases were 147, 190, and 176 seconds (mean time 171 ± 22 seconds).

Case 1

A 13-year-old 55.5 kg female was referred to the CCL for a severe native coarctation of the aorta with an arm-leg cuff PSG of 56 mmHg with upper extremity hypertension (146/52 mmHg). Catheterization revealed a discrete, severe coarctation distal to the left subclavian artery. PSG was 41 mmHg with a TDCO of 4.7 L/min (Table I), and the CFD processor predicted a PSG of 40 mmHg. The coarctation was treated with a 36 mm long Cheatham Platinum (CP) stent (NuMED, Hopkinton, NY) mounted on a 12 mm Z-Med II-X balloon catheter (NuMED,

Hopkinton, NY). The residual PSG across the arch was 14 mmHg, and virtual stenting predicted a residual PSG of 10 mmHg (Figure 2 and Table II).

Case 2

A 16-year-old 69.6 kg male came to the CCL for treatment of a native coarctation of the aorta, due to an arm-leg cuff PSG of 50 mmHg with upper extremity hypertension (150/82 mmHg). He also had a bicuspid aortic valve, mild aortic regurgitation, and a dilated aortic root. Catheterization showed a moderate, discrete coarctation distal to the left subclavian artery with a PSG of 29 mmHg and TDCO of 5.7 L/min. CFD predicted a PSG of 29 mmHg. The coarctation was treated with a 45 mm long CP stent mounted on a 15 mm Z-Med II-X balloon catheter. The residual PSG was 3 mmHg, and, after virtual stenting, the PSG was computed as 2 mmHg (Figure 3 and Table II).

Case 3

A 10-year-old 34.8 kg female underwent catheterization for a native coarctation of the aorta, due to an arm-leg cuff PSG of 32 mmHg without upper extremity hypertension. A mild, discrete coarctation in the mid-thoracic descending aorta resulted in a PSG of 19 mmHg with a TDCO of 3.9 L/min. CFD computed a PSG of 18 mmHg. The coarctation was treated with a 39 mm long covered CP stent mounted on a 16 mm Balloon in Balloon catheter (NuMED, Hopkinton, NY). There was no residual gradient from ascending aorta to descending aorta at catheterization and or in the model with virtual stenting (Figure 4 and Table II).

Discussion

Since the 1990s, MRI-based CFD advanced from a preclinical modality to clinical application by evaluating pathophysiology, surgical and catheter-based treatment planning, and outcome prediction. However, clinical data to prove the accuracy of the data obtained from CFD in congenital heart disease are still limited. Aside from case reports, two studies have compared catheter-based and CFD-based gradients before and after aortic stenting and virtual stenting, respectively. First, Goubergrits *et al* evaluated 13 patients who underwent catheterization and preceding MRI, 1 day to 4 weeks apart, for coarctation of the aorta (11). MRI included 3D whole-heart and flow-sensitive 4D velocity-encoded sequences (Gyrotools, Zurich, Switzerland). CFD assessments were performed using Fluent® 6.3.26 (Ansys, Canonsburg, PA), and the post-treatment aortic geometry was virtually reconstructed from x-ray images. Pre-stent PSGs measured by catheter- and MRI-based CFD correlated significantly with a correlation coefficient of 0.97 and an absolute error of -0.5±0.33 mmHg. Post-stent PSGs also correlated significantly with a correlation coefficient of 0.87 and absolute error of 3.0±2.91 mmHg (11).

Second, Ralovich *et al* investigated data sets from 6 coarctation patients who had undergone pre- and post-intervention MRI and catheterizations (10). Using MRI-based CFD and virtual stenting, there was good agreement between CFD computed PSGs and catheter PSGs with an average absolute error of 2.38±0.82 mmHg (pre-stenting), 1.10±0.63 mmHg (post-stenting), and 4.99±3.00 mmHg (virtual stenting).

To date, 3DRA-based CFD has been used clinically to understand the hemodynamics of brain aneurysms and to aid in treatment planning but has not been used in cardiac disease. Because of its high spatial resolution, low sensitivity to patient motion, and low visibility of bone, 3DRA has

been used as the imaging gold standard when comparing CFD using MRI and CTA (13). Our first use of this imaging modality to perform cardiac CFD not only shows feasibility but also begins to validate its hemodynamic computations with catheter-based measurements, as all the gradients were within 5 mmHg of absolute error.

While CFD predicted the gradients with minimal absolute error, the post-stenting absolute pressures were not predicted accurately in all cases. The personalization for both the pre- and virtual post-stenting CFD based computations was performed using solely pre-stenting hemodynamic measurements, in order to mimic predictive modeling used real-time in the catheterization laboratory, during which only pre-stent hemodynamics would be available. For example, in Case #1, the patient's hemodynamics changed quite significantly between the pre- and post-stent settings (Table I) with the ascending aortic pressure and TDCO decreasing after stent placement. Despite using the pre-stent hemodynamics in the model, a prediction error of 4 mmHg indicated that the PSG prediction was quite robust and that its accuracy was only marginally affected by the change in post-stent hemodynamics.

3DRA-based cardiac CFD is the first step to perform virtual interventions real-time in the CCL and to allow CFD to guide management decisions during cardiac catheterization. Previous cardiac predictive modeling has used pre-procedural MRI or CTA (14,15). Our novel workflow could allow for CFD-guided personalized management decisions even when pre-procedural advanced imaging is not performed (14,15).

Limitations

The small prediction error (<5 mmHg) is one limitation of CFD, and a detailed uncertainty quantification analysis is planned for future studies. Error can come from modeling assumptions, anatomical reconstruction errors, inaccurate elastic wall modeling, and inaccuracies in the physiological measurements, such as thermodilution cardiac output. The reduced-order multiscale model is also limited by its inability to produce 3D streamlines, vortices, and wall shear stress. It was chosen for performing the blood flow computations, mainly due to the significantly reduced computation time, with an aim of running the calculations real-time, while the patient is on the catheterization table.

Conclusion

The ability to have patient-specific predictive modeling with hemodynamic assessment in the CCL will allow clinical decisions regarding stent therapy to be based on robust data, as opposed to guessing and assumptions, as it is done now. This may revolutionize the way we make clinical decisions and significantly improve care, if this can be done real-time during the catheterization. Widespread use of this technology will require large-scale studies to assure reliability and validity and to move CFD assessment into the CCL.

References

1. Baumgartner H, Bonhoeffer P, De Groot N, de Haan F, Deanfield J, Galie N, Gatzoulis M, Gohlke-Baerwolf C, Kaemmerer H, Kilner P, Meijboom F, Mulder B, Oechslin E, Oliver J, Serraf A, Szatmari A, Thaulow E, Vouhe P, Walma E. ESC Guidelines for the management of grown-up congenital heart disease (new version 2010). *Eur Heart J* 2010;31:2915–2957. doi: 10.1093/eurheartj/ehq249.

2. Bouchart F, Dubar A, Tabley A, Litzler P, Haas-Hubscher C, Redonnet M, Bessou J, Soyer R. Coarctation of the Aorta in Adults: Surgical Results and Long-Term Follow-up. *Ann Thorac Surg* 2000;79:1483-1488.

3. Feltes T, Bacha E, Beekman R, Cheatham J, Feinstein J, Gomes A, Hijazi Z, Ing F, de Moor M, Morrow W, Mullins C, Taubert K, Zahn E. Indications for cardiac catheterization and intervention in pediatric cardiac disease: a scientific statement from the American Heart Association. *Circulation* 2011;123:2607-2652. doi: 10.1161/CIR.0b013e31821b1f10.

4. Meadows J, Minahan M, McElhinney DB, McEnaney K, Ringel R; on behalf of the COAST Investigators. Intermediate Outcomes in the Prospective, Multicenter Coarctation of the Aorta Stent Trial (COAST). *Circulation* 2015;131:1656-1664. doi: 10.1161/CIRCULATIONAHA.114.013937.

5. Quennelle S, Powell A, Geva T, Prakash A. Persistent aortic arch hypoplasia after coarctation treatment is associated with late systemic hypertension. *J Am Heart Assoc* 2015;4:1-8. doi: 10.1161/JAHA.115.001978.

6. Lee BK. Computational Fluid Dynamics in Cardiovascular Disease. *Korean Circ J* 2011;41:423-430. doi: 10.4070/kcj.2011.41.8.423.

7. Pennati G, Corsini C, Hsia T-Y, Migliavacca F, for the Modeling of Congenital Hearts Alliance (MOCHA) Investigators. Computational fluid dynamics models and congenital heart diseases. *Front Pediatr* 2013;1:1-7. doi: 10.3389/fped.2013.00004.

8. Morris PD, Narracott A, von Tengg-Kobligk H, Soto DAS, Hsiao S, Lungu A, Evans P, Bressloff NW, Lawford PV, Hose DR, Gunn JP. Computational fluid dynamics modelling in cardiovascular medicine. *Heart* 2016;102:18-28. doi: 10.1136/heartjnl-2015-308044

9. Koo B, Erglis A, Doh J, Daniels D, Jegere S, Kim H, Dunning A, DeFrance T, Lansky A, Leipsic J, Min J. Diagnosis of Ischemia-Causing Coronary Stenoses by Noninvasive Fractional Flow Reserve Computed From Coronary Computed Tomographic Angiograms Results From the Prospective Multicenter DISCOVER-FLOW (Diagnosis of Ischemia-Causing Stenoses Obtained Via Noninvasive Fractional Flow Reserve) Study. *J Am Coll Cardiol* 2011;58:1989–1997. doi: 10.1016/j.jacc.2011.06.066.

10. Ralovich K, Itu L, Vitanovski D, Sharma P, Ionasec R, Miahlef V, Krawtschuk W, Zheng Y, Everett A, Pongiglione G, Lenoardi B, Ringel R, Navab N, Heimann T, Comaniciu D. Noninvasive hemodynamic assessment, treatment outcome prediction and follow-up of aortic coarctation from MR imaging. *Med Phys* 2015;42:2143-56. doi: 10.1118/1.4914856.

11. Goubergrits L, Riesenkampff E, Yevtushenko P, Schaller J, Kertzscher U, Hennemuth A, Berger F, Schubert S, Kuehne T. MRI-Based CFD for Diagnosis and treatment Prediction: Clinical Validation Study in Patients with Coarctation of the Aorta. *J Magn Reson Imaging* 2015;41:909-916. doi: 10.1002/jmri.24639

12. Itu L, Sharma P, Ralovich K, Mihalef V, Ionasec R, Everett A, Ringel R, Kamen A, Comaniciu D. Non-invasive hemodynamic assessment of aortic coarctation: validation with in vivo measurements. *Ann Biomed Eng* 2013;41:669–681. doi: 10.1007/s10439-012-0715-0.

13. Ren Y, Chen G, Liu Z, Cai Y, Lu G, Li Z. Reproducibility of image-based computational models of intracranial aneurysm: a comparison between 3D rotational angiography, CT angiography and MR angiography. *BioMed Eng OnLine* 2016;15:50-64. doi: 10.1186/s12938-016-0163-4.

14. Capelli C, Sauvage E, Giusti G, Bosi GM, Ntsinjana H, Carminati M, Derrick G, Marek J, Khambadkone S, Taylor AM, Schievano S. Patient-specific simulations for planning treatment in congenital heart disease. *Interface Focus* 2018;8:20170021. doi: 10.1098/rsfs.2017.0021.

15. Kwon S, Feinstein JA, Dholaki RJ, LaDisa JF. Quantification of local hemodynamic alterations caused by virtual implantation of three commercially-available stents for the treatment of aortic coarctation. *Pediatr Cardiol* 2014;35:732-740. doi: 10.1007/s00246-013-0845-7.

Figure Legends

Figure 1: 3D Rotational Angiography Computational Fluid Dynamics Workflow: (a) 3D rotational angiogram (arrow showing discrete coarctation), (b) segmentation, (c) final 3D segmented model, (d) boundary conditions added, (e) gradient prediction, (f) virtual stent implantation with boundary conditions, and (g) post-stent gradient prediction

Asc, Ascending; Desc, Descending

Figure 2: Case 1 (a) Dyna CT reconstruction and (b) pressure predictions pre-stent and (c) post-stent

Asc, Ascending; Desc, Descending; CFD, Computational Fluid Dynamics; Meas, Measured

Figure 3: Case 2 (a) Dyna CT reconstruction and (b) pressure predictions pre-stent and (c) post-stent

Asc, Ascending; Desc, Descending; CFD, Computational Fluid Dynamics; Meas, Measured

Figure 4: Case 3 (a) Dyna CT reconstruction and pressure predictions (b) pre-stent and (c) post-stent

Asc, Ascending; Desc, Descending; CFD, Computational Fluid Dynamics; Meas, Measured

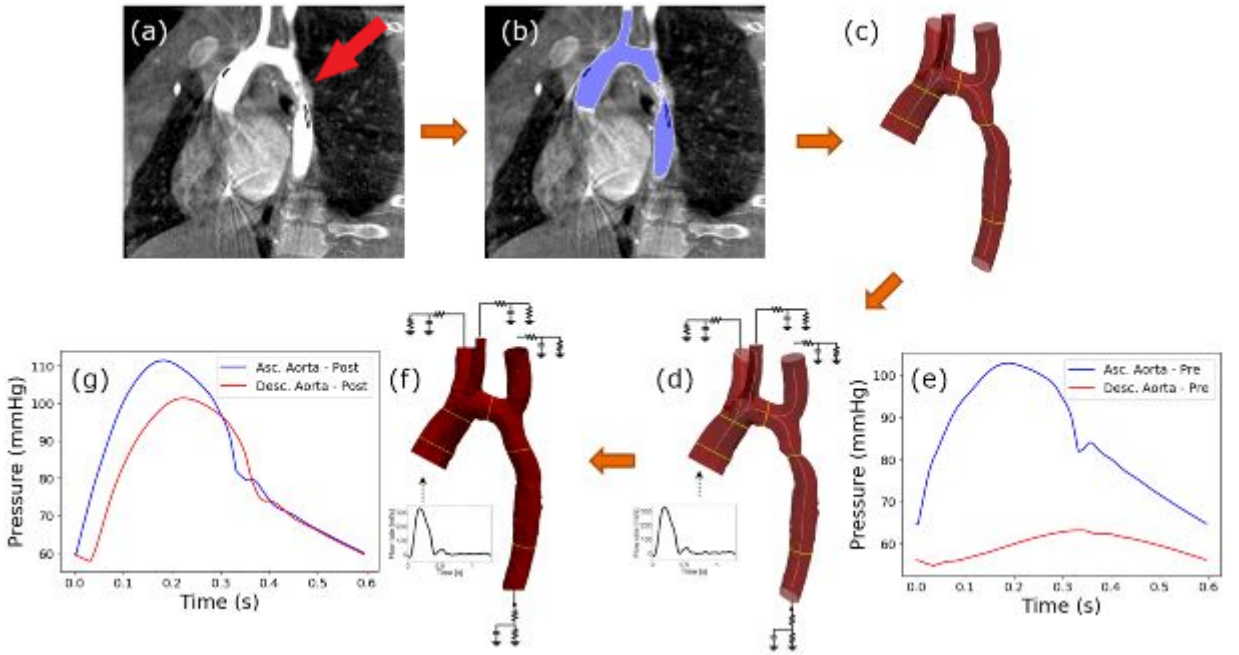

CCD_28507_Figure 1.tiff

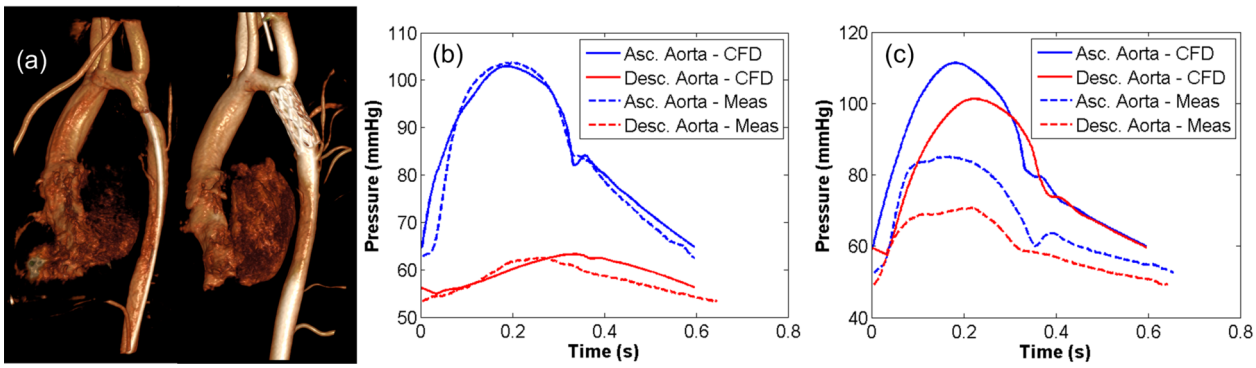

CCD_28507_Figure 2.tif

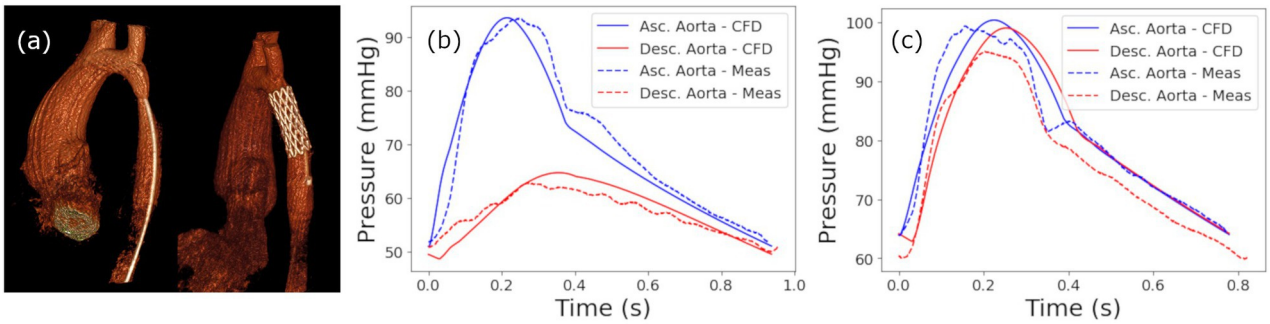

ccd_28507_figure 3.eps

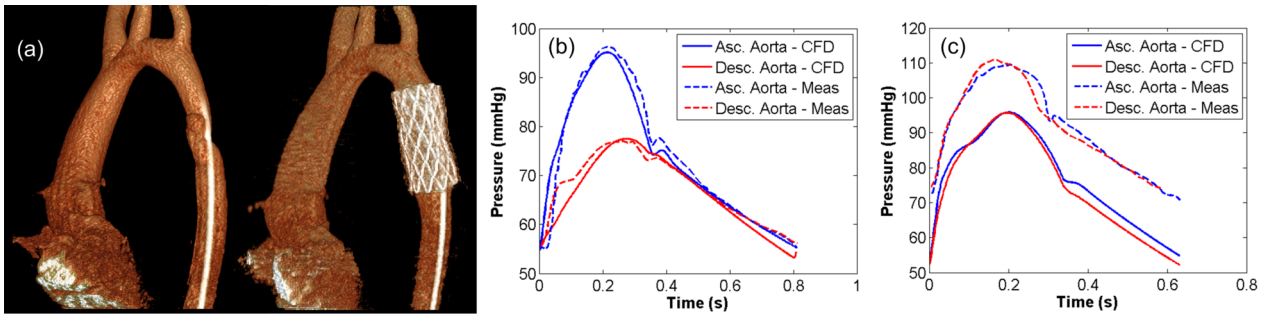

CCD_28507_Figure 4.tif

Table I. (A) Pre-stent and (B) post-stent physiologic and anatomical parameters measured at catheterization

A. Pre-stent

Case	AAo BP [mmHg]	DAo BP [mmHg]	TDCO* [l/min]	Heart rate [bpm]	Minimum coarctation diameter [mm]	AAO diameter [mm]
1	104/62	63/53	4.7	101	4.4	16
2	92/51	63/51	5.7	64	6.8	40
3	96/54	77/56	3.9	74	5.9	17

B. Post-stent

Case	AAo SBP [mmHg]	DAo SBP [mmHg]	TDCO* [l/min]
1	85/52	71/48	3.7
2	100/54	97/61	6.4
3	109/71	110/74	5.7

AAo, Ascending aorta
DAo, Descending aorta
BP, Blood pressure
TDCO, thermodilution cardiac output
*Pre-stent TDCO was used for post-stent CFD in order to simulate real-time workflow in the cardiac catheterization laboratory

Table II. Pre-stent and post-stent peak systolic gradients (mmHg) measured by direct catheterization pullback (ascending aortic systolic pressure – descending aortic systolic pressure) and by Computational Fluid Dynamics

	Pre-Stent		Post-Stent	
	Measured	**CFD***	**Measured**	**CFD***
Case 1	41	40	14	10
Case 2	29	29	3	2
Case 3	19	18	0	0

*CFD, Computational Fluid Dynamics